AUTHOR(S):

Tanaka, Motomu; Thoma, Judith; Poisa-Beiro, Laura; Wuchter, Patrick;
Eckstein, Volker; Dietrich, Sascha; Pabst, Caroline; Müller-Tidow,
Carsten; Ohta, Takao; Ho, Anthony D.

京都大学学術情報リポジトリ
KURENAI 紅
Kyoto University Research Information Repository

Contents lists available at ScienceDirect

Cells & Development

journal homepage: www.journals.elsevier.com/cells-and-development

Physical biomarkers for human hematopoietic stem and progenitor cells

Motomu Tanaka [a,b,*], Judith Thoma [a,1], Laura Poisa-Beiro [c,1], Patrick Wuchter [c,2],
Volker Eckstein [c,1], Sascha Dietrich [c,1], Caroline Pabst [c,1], Carsten Müller-Tidow [c,1],
Takao Ohta [b,1], Anthony D. Ho [b,c,d,*]

[a] Physical Chemistry of Biosystems, Institute of Physical Chemistry, INF253, Heidelberg University, 69120 Heidelberg, Germany
[b] Center for Integrative Medicine and Physics, Institute for Advanced Study, Kyoto University, 606-8501 Kyoto, Japan
[c] Department of Medicine V, Heidelberg University, INF410, 69120 Heidelberg, Germany
[d] Molecular Medicine Partnership Unit Heidelberg, European Molecular Biology Laboratory (EMBL), Heidelberg University, 69120 Heidelberg, Germany

ARTICLE INFO

ABSTRACT

Adhesion of hematopoietic stem and progenitor cells (HSPCs) to the bone marrow niche plays critical roles in the maintenance of the most primitive HSPCs. The interactions of HSPC−niche interactions are clinically relevant in acute myeloid leukemia (AML), because (i) leukemia-initiating cells adhered to the marrow niche are protected from the cytotoxic effect by chemotherapy and (ii) mobilization of HSPCs from healthy donors' bone marrow is crucial for the effective stem cell transplantation. However, although many clinical agents have been developed for the HSPC mobilization, the effects caused by the extrinsic molecular cues were traditionally evaluated based on phenomenological observations. This review highlights the recent interdisciplinary challenges of hematologists, biophysicists and cell biologists towards the design of defined *in vitro* niche models and the development of physical biomarkers for quantitative indexing of differential effects of clinical agents on human HSPCs.

Introduction

Functions of somatic stem cells are tightly controlled by the balance between self-renewal and differentiation. This balance is in turn regulated by interactions between stem cells and their microenvironment, the so-called "niche" (Moore and Lemischka, 2006). In the case of hematopoietic stem and progenitor cells (HSPCs), the adhesion to the bone marrow niche has been shown to maintain the dormancy of the most primitive HSPCs (Fig. 1A). Ample evidence has indicated that mesenchymal stromal cells, osteoblasts, and endothelial cells function as the surrogate niche in the bone marrow, supporting HSPC maintenance (Lapidot et al., 2005; Mendelson and Frenette, 2014; Ho and Wagner, 2007; Morrison and Scadden, 2014). It has been reported that the coculture of HSPCs and mesenchymal stromal cells increases proliferation and maintenance of HSPCs (Walenda et al., 2010; Wuchter et al., 2022). Furthermore, HSPCs are frequently found in the vicinity of blood vessels, suggesting that HSPCs might be maintained in a vascular niche by endothelial cells. (Kiel et al., 2005; Ding et al., 2012) To date, several

key molecular interactions between HSPCs and their cellular niche have been identified. Using mouse models, it has been shown that long-term HSPCs adhere to spindle-shaped osteoblasts expressing N-cadherin, suggesting that the homophilic N-cadherin interactions are involved in the maintenance of dormancy (Zhang et al., 2003; Calvi et al., 2003). Wein et al. showed that the N-cadherin expressed on HSPCs mediates interaction with mesenchymal stem cells (Fig. 1B) (Wein et al., 2010), and Méndez-Ferrer et al. demonstrated that mesenchymal stem cells expressing nestin physically associate with HSPCs and act as niche cells (Méndez-Ferrer et al., 2010). The overexpression of N-cadherin in HSPCs further resulted in the enhancement of cytoadhesion and the suppression of HSPC division *in vitro*, suggesting that N-cadherin-mediated adhesion supports maintenance of long-term pools of HSPCs (Hosokawa et al., 2010). Another key molecular axis is the interaction between stromal cell-derived factor 1α (SDF1α) and its receptor CXCR4, which has been shown to regulate the mobilization of HSPCs (Möhle et al., 1998; Ponomaryov et al., 2000; Lapidot and Kollet, 2002; Dar et al., 2005). SDF1α is a multifunctional cytokine that serves as a

---

* Corresponding authors at: Center for Integrative Medicine and Physics, Institute for Advanced Study, Kyoto University, 606-8501 Kyoto, Japan.
E-mail addresses: tanaka@uni-heidelberg.de (M. Tanaka), a_d_ho@msn.com (A.D. Ho).
[1] Present address: Department of Hematology, Oncology, and Clinical Immunology, Universitätsklinikum Düsseldorf, 40225 Düsseldorf, Germany.
[2] Present address: Institute of Transfusion Medicine and Immunology, Medical Faculty Mannheim, Heidelberg University, German Red Cross Blood Service Baden-Württemberg – Hessen, 68167 Mannheim, Germany.

chemoattractant for HSPCs, which plays a major role in the trafficking of HSPCs between the bone marrow niche and the vascular niche (Aiuti et al., 1997). Notably, SDF1α can be found not only as a soluble proteins in the marrow fluid but also as an immobilized molecule on the surface of mesenchymal stromal cells (Peled et al., 1999).

The HSPC-niche interactions have been drawing increasing attentions due to the clinical relevance. A prominent example is acute myeloid leukemia (AML), which is a highly lethal, clonal disorder (Lowenberg et al., 1999). In AML patients, HSPCs lose their normal capability for the lineage commitment to granulocytes and monocytes. This leads to the accumulation of undifferentiated leukemia blasts, resulting in pancytopenia (Lowenberg et al., 1999). Leukemia blasts are derived from leukemia initiating cells (LIC). The latter are protected from cell division by adhesion to the bone marrow niche and hence are resistant to the cytotoxic effect by chemotherapy (McCulloch, 1983; Bonnet and Dick, 1997). Therefore, the mobilization of LIC from the bone marrow niche is of highly clinical relevance to eliminate the source of AML (Ishikawa et al., 2007; Lane et al., 2009; Valent et al., 2012).

Transplantation of peripheral HSPC has induced a more rapid reconstitution of bone marrow function and has largely replaced bone marrow-derived cells since the 1980s (To et al., 1997; Copelan, 2006; Duong et al., 2014; Passweg et al., 2016). As the mobilization of HSPCs from healthy donors' bone marrow is crucial for the effective collection of peripheral HSPCs for transplantation, a better understanding of homing and mobilization of normal HSPC is of clinical significance (Lapidot et al., 2005).

To date, many clinical agents have been examined to achieve the efficient mobilization of HSPC from the bone marrow of healthy donors. G-CSF has widely been used over the past 30 years for the treatment of AML patients, because of its capability to mobilize HSPCs from the bone marrow by inducing the secretion of extracellular proteases (Petit et al., 2002; Welte, 2014). However, among those who are intended for autologous transplantation, about 10–15 % of patients have difficulties in mobilizing an adequate amount of HSPC for transplantation (Wuchter et al., 2010). Thus, there is an increasing demand for new and highly effective mobilizing reagents for a better AML therapy. For example, plerixafor (AMD3100) (Broxmeyer et al., 2005; Pusic and DiPersio, 2010) has been proven highly effective for the mobilization of CD34^{+} cells for autologous transplantations, especially in poor mobilizing patients (DiPersio et al., 2009; Fruehauf et al., 2009; Cheng et al., 2015). Although it was designed and regarded as a CXCR4-antagonist, the mechanism of action is not as simple as initially considered because clinical agents, like naturally occurring compounds, do not target only one molecular site (Ludwig et al., 2014). Conversely, they often interact with and affect various molecules and pathways, which might cause undesirable side effects. Both plerixafor and SDF1α generate phosphorylation of MEK1/2 and ERK1/2, which results in cell proliferation. On the other hand, plerixafor leads to a sustained release of cAMP, while SDF1α induces a surge of cAMP. One of the strategies taken in recent years is the perturbation assay combined with high throughput microscopy (Boutros et al., 2015). This is based on the combination of the image-based screening and the perturbations (RNA interference, small molecules, and mutations) and opens a large potential for gaining systematic insights into cancer cell vulnerabilities and changes in protein localization.

In vitro studies on how clinical agents and naturally occurring chemokines affect the interactions between human HSPCs and the microenvironment face numerous challenges. The effects caused by the extrinsic molecular cues were traditionally evaluated based on phenomenological observations. This might impede researchers from performing the experiments under biologically relevant conditions. For example, the previous *in vitro* experiments on HSPC-MSC adhesion were performed at [SDF1α] = 500 ng/mL, which is by two orders of magnitude higher than the physiological level (5 ng/mL) as no measurable
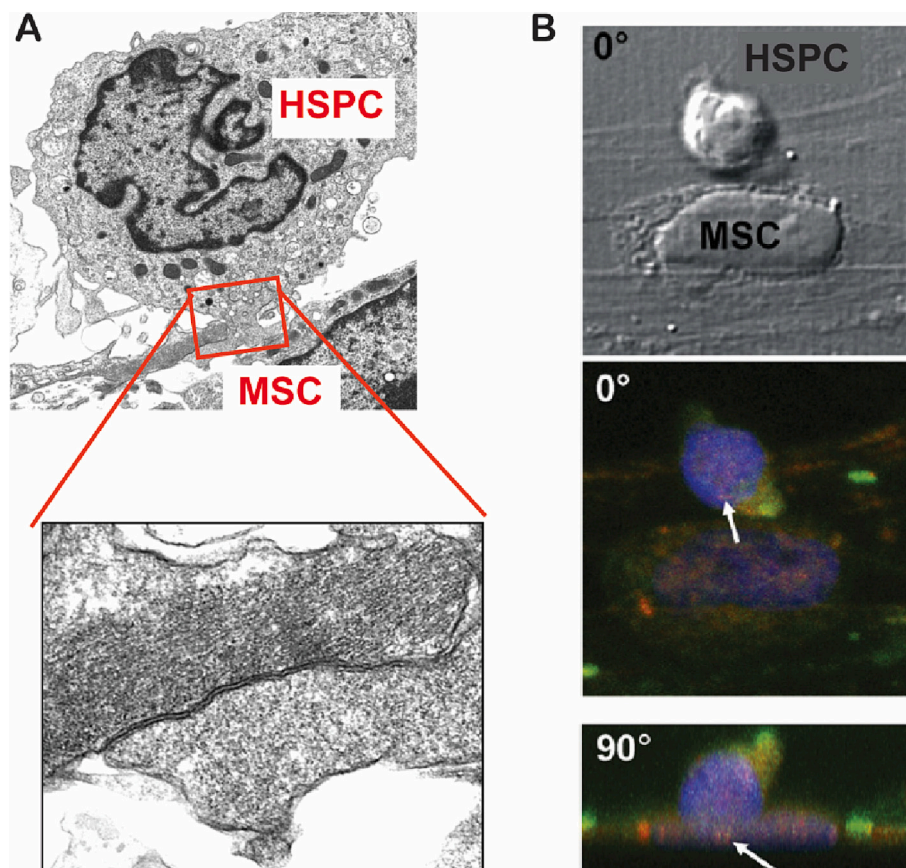

Fig. 1. Adhesion of hematopoietic stem and progenitor cell (HSPC) to mesenchymal stromal cell (MSC) plays key roles in maintenance of dormancy. (A) Electron micrograph of HSPC-MSC junction. (Ho AD & Franke W, unpublished results). Differential interference contrast image of co-cultured HSPC and MSC (*t* = 48 h). 3D reconstructed confocal fluorescence micrographs from the bottom (0°) and side (90°). Blue; cell nucleus, red, β-catenin, green; N-cadherin. White arrows indicate co-localization of β-catenin and N-cadherin near the cell-cell contact. Adapted from (Wein et al., 2010). (For interpretation of the references to colour in this figure legend, the reader is referred to the web version of this article.)

influence could be observed at lower concentrations. Moreover, despite of numerous reports demonstrating that the adhesion of HSPC to mesenchymal stromal cells, methods to quantitatively assess adhesiveness could not be performed. A commonly used assay utilizes a feeder layer of human mesenchymal stromal cells either on two/dimensional culture dish surfaces or in three-dimensional hydrogels (Wagner et al., 2007; Monika et al., 2012). After seeding or co-culturing HSPCs, the number of adhered HSPCs was counted after flipping the chamber upside-down (Fig. 2A) (Fruehauf et al., 2009; Voermans et al., 1999). Although the co-culture of HSPCs and mesenchymal stromal cells enables to mimic the bone marrow niche, this strategy has two drawbacks. First, the expression level of ligands, such as N-cadherin and SDF1α, on the surface of surrogate cells can hardly be defined or controlled. This makes it difficult to discriminate the contributions of differential molecular interactions. Second, this kind of assay can discriminate whether cells adhere or not but cannot compare the dimension of cell adhesion in a quantitative manner.

There is an urgent need for well-defined, *in vitro* niche models for adhesion between human HSPC and their niche to quantitatively and precisely assess the interplay between differential molecular interactions and to evaluate the differential effects of extrinsic factors. This review highlights some of the recent achievements in this respect, involving interdisciplinary collaborations among hematologists, biophysicists and cell biologists.
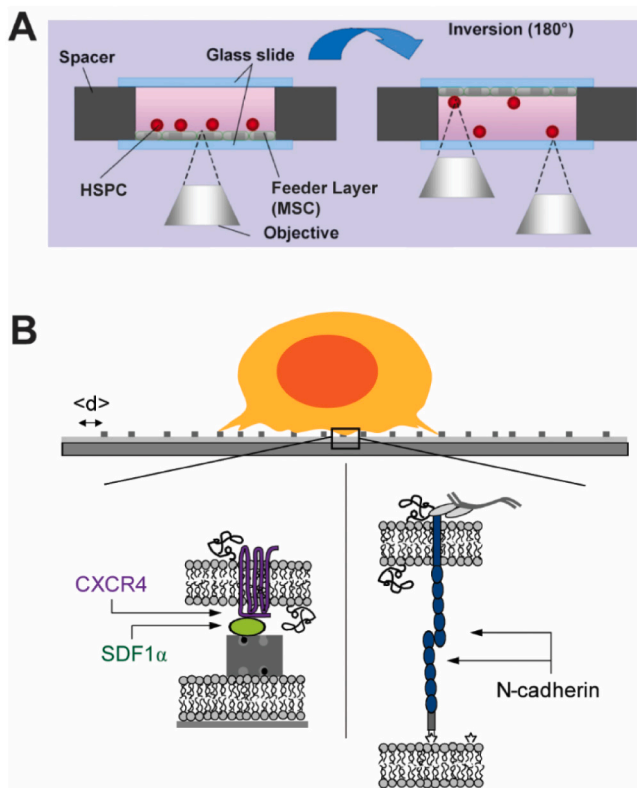

Fig. 2. *In vitro* models of HSPC-MSC interactions in bone marrow niche. (A) Co-culture of HSPC and MSC. The number of adhered HSPCs on the MSC feeder layer is counted after flipping the chamber upside-down. Adapted from (Wagner et al., 2007). (B) Surrogate surface model based on "supported membranes". Roles of differential ligands (SDF1α and N-cadherin) can be dissected by the precise control of intermolecular distance <d> with nm accuracy (Tanaka and Sackmann, 2005; Balta et al., 2019). Modified and adapted from (Monzel et al., 2018).

Quantitative model of bone marrow niche based on "supported membranes"

Bilayer lipid membranes are the main constituent of cell membranes, which provide quasi two-dimensional matrix for various lipids and proteins. Planar lipid membranes deposited on planar substrates, called "supported membranes" have been used as a well-defined model of cell membranes (Sackmann, 1996; Tanaka and Sackmann, 2005; Tanaka, 2019). It has been shown that the fluid nature of lipid membranes is sustained, which further allows for the lateral diffusion and self-assembly of functional molecules. To model the surrogate surface of niche cells, one can functionalize the surface of supported membranes with ligand molecules, such as N-cadherin and SDF1α (Fig. 2B). By using recombinant proteins coupled with histidine or biotin tags, the proteins can be selectively harnessed on the membrane surface by binding to synthetic anchor lipids with nitrotriacetic acid (NTA) or biotin head groups. The average intermolecular distance between the ligand molecules $\langle d \rangle$ can be controlled at nm accuracy with the molar fraction of anchor lipids χ by tuning the self-assembly:

$$\langle d \rangle = \sqrt{A_{\text{lipid}}/\chi},$$

where A_{lipid} is the area occupied by one lipid molecule, $A_{\text{lipid}} = 60\text{–}70 \text{ Å}^2$ (Fröhlich et al., 2021). This means that $\chi = 0.005$ coincides with $\langle d \rangle = 11\text{–}12$ nm, while $\chi = 0.001$ with 24–26 nm. The selective interaction with anchor lipids, whose dissociation constants are in the order of 10^{-12} M or smaller, realizes a statistically reliable model to study cell adhesion.

Using this surrogate surface, one can quantitatively evaluate the cell adhesion function on different levels (Burk et al., 2015). On the ensemble level, one can assess the surface density of HSPCs after removing non-adhered cells, which is similar to the commonly used "flipping" or "washing" assays. As summarized in Fig. 3A (red), an increase in the average lateral distance $\langle d \rangle$ of SDF1α resulted in a significant decrease in the fraction of adherent HSC χ, indicating the transition from the "bound" state (close to 100 % of cells are adherent) to "unbound" state (close to the base line). The χ *vs.* $\langle d \rangle$ plot can be fitted with the empirical Hill equation:

$$\chi = \chi_{\min} + \frac{\chi_{\max} - \chi_{\min}}{1 - \left(\langle d \rangle / \langle d^* \rangle\right)^n}.$$

$\chi_{\min}$ and $\chi_{\max}$ are the minimum and maximum levels, $\langle d^* \rangle$ is the characteristic inter-ligand distance for transition and n is the Hill coefficient. The unbinding transition could be characterized by the critical distance $\langle d^* \rangle \approx 27$ nm and the cooperativity coefficient $n \approx 3$, respectively. In contrast, the corresponding results for N-cadherin (blue) exhibited a broader tail to a large intermolecular distance $\langle d^* \rangle \approx 50$ nm with a cooperativity coefficient $n \approx 2$. The results suggested that HSPCs sensitively detected nano-scale changes in $\langle d \rangle$. Moreover, the obtained Hill coefficient ($n > 1$) on both surfaces indicated that the HSPCs adhesion to the surrogate niche is a cooperative reaction. HSPCs seeded on a pure phospholipid membrane showed no sign of adhesion (Fig. 3A, black), confirm that the adhesion of HSPCs to the *in vitro* model niche is specific. This approach could be applied for the discrimination of HSPCs from healthy donors and leukemia blasts from AML patients (Burk et al., 2015). The adhesion of leukemia blasts harvested from the peripheral blood of an AML patient was compared with that of peripheral blood HSPCs from a healthy donor. The fraction of adherent leukemia blasts of an AML patient (88 %) was about 1.5 times higher than that of peripheral blood HSPCs of a helthy donor (55 %), demonstrating that the *in vitro* surrogate surface can discriminate leukemia blasts and healthy HSPCs.

Yet, the determination of the fraction of adherent cells by such an "ensemble counting" still does not allow for a clear discrimination between strong and weak adhesion. On the single cell level, one can
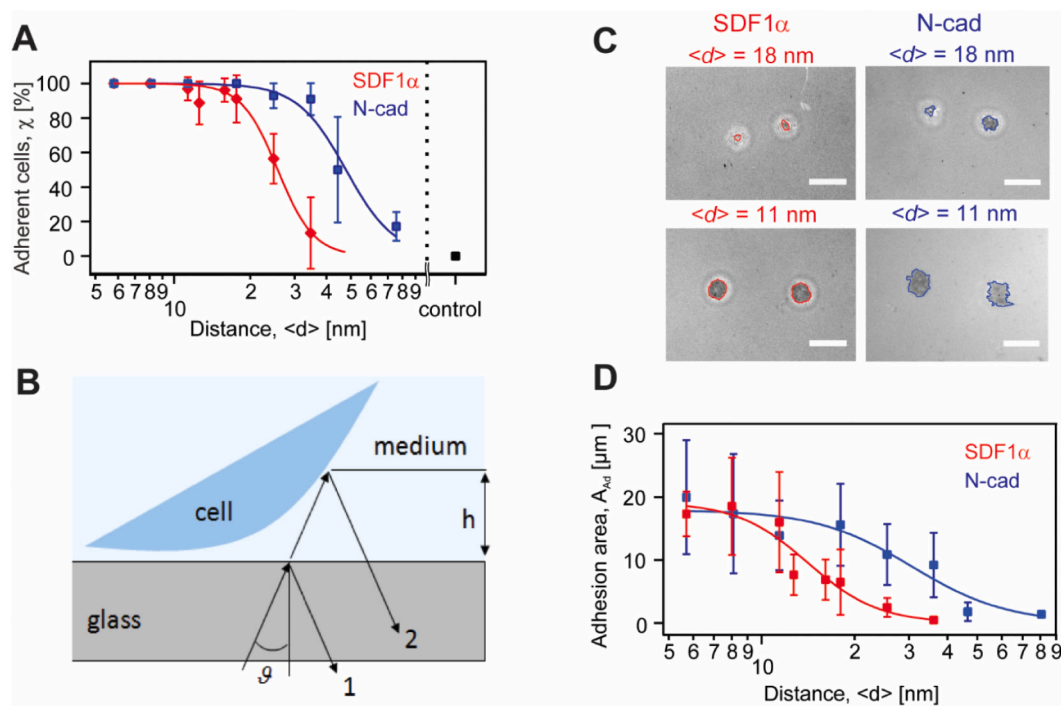
Fig. 3. Quantitative assessment of adhesion of HSPCs on membrane-based surrogate surfaces. (A) Fraction of adhered cells χ_{adh} plotted as inter-ligand distance on the surface $<d>$. Red; SDF1α, blue; N-cadherin. Black symbol is the negative control on pure lipid membranes. Solid lines coincide with the empirical fitting with Hill's eq. (B) Scheme of microinterferometry. Intensity of light refected at substrate/medium and medium/membrane interfaces can be used to calculate the local membrane-substrate distance. The adhesion contact is seen black due to distructive interference. (C) Overlays of phase contrast and microinterferometry. Adhesion contacts determined by interferometry are highlighted by solid lines. Scale bars: 10 μm. (D) Area of tight adhesion A_{adh} plotted *versus* $<d>$. Red; SDF1α, blue; N-cadherin. Adapted from (Burk et al., 2015). (For interpretation of the references to colour in this figure legend, the reader is referred to the web version of this article.)

precisely determine the adhesion contact areas for individual cells by using non-invasive micro-interferometry, called reflection interference contrast microscopy (Fig. 3B) (Fröhlich et al., 2021; Kaindl et al., 2012). As shown in Fig. 3C, the phase contrast imaging is useful for the comparison of global cell morphology, while micro-interferometry highlights the differences in size and shape of the adhesion zones (Fröhlich et al., 2021; Burk et al., 2015).

Fig. 3D represents the calculated area of tight adhesion per cell plotted as a function of $\langle d \rangle$ for SDF1α (red) and N-cadherin (blue). The clear discrimination in the area of tight adhesion at $\langle d \rangle \leq 18$ nm for SDF is distinct from the ensemble counting data, in which the cells were merely classified either as "adherent" or "non-adherent". This might cause the apparent differences in the unbinding transition to a smaller critical distance, $\langle d^* \rangle = 14$ nm for SDF1α and 31 nm for N-cadherin, obtained by replacing χ to A in Hill equation. Note that these *in vitro* experiments are suited for the quantification of cell adhesion strength mediated *via* ligand-receptor interactions on relatively shorter time scale ($t \leq 10$ h), because the model with reduced number of components might not be able to support biochemical reactions on longer time scale.

High throughput quantification of cytoadhesiveness using ultrasonic pressure waves

Common approaches to assess the mechanical significance of cell adhesion include pulling with micropipette suction (Sung et al., 1986; Evans et al., 1995; Shao et al., 2004), pulling of cells with optical tweezers (Thoumine et al., 2000; Neuman and Nagy, 2008), or scratching/pulling of cells with atomic force microscopy (AFM) (Yamamoto et al., 1998; Friedrichs et al., 2013). However, despite of their major progresses owing to their unique advantages, these techniques have several fundamental drawbacks. First, unless one can trap/pull the cell directly, the pulling of cells always requires tracer particles/

probes, such as chemically functionalized latex particles strongly binding to the cell. Note that the probe-cell binding must be stronger than cell adhesion to measure the adhesion force. Such strong probe-cell interactions, such like the firm attachment of one cell on an AFM cantilever, induces the remodeling of actin cytoskeletons. The suction by a micropipette also causes the cell deformation, which is also followed by the remodeling of cytoskeletons. Second, the possibility of cells to react/remodel in response to the mechanical manipulations (suction, scratching and pulling) during the measurements. As shown by Merkel et al., the bond rupture force between ligand and receptor molecules depends on the loading/pulling rate almost exponentially (Merkel et al., 1999).

We developed a novel experimental technique to measure the mechanical significance of cell adhesion using pressure waves induced by intensive picosecond (ps) laser pulses (Fig. 4A) (Burk et al., 2015; Yoshikawa et al., 2011; Rieger et al., 2015). The pressure that can be exerted on a cell ($\sim$ MPa) is approximately six orders of magnitude larger than the typical force range achieved with optical traps (Finer et al., 1994) and magnetic tweezers (Bausch et al., 1999), which are strong enough to cause cell detachment in a non-invasive manner. As the applied pressure can be calibrated from knowledge of the laser energy and the distance between the focal point and the target, the critical pressure required for cell detachment can be determined. In contrast to the above-mentioned techniques, this method is a probe-free, non-invasive technique that enables reliable statistics from many cells with a high throughput, typically $N > 100$ cells/h. Moreover, a pressure wave traveling at the supersonic velocity (approximately 1640 m·s^{-1}) has the full width at a half maximum of ≈ 80 ns. Here, the dependence of detachment force on the loading rate and the biochemical response of cells to the external force (*e.g.* remodeling of cytoskeletons) are negligible, because the cell deformation by shock waves should be predominantly elastic within such a short time frame (Engelhardt and
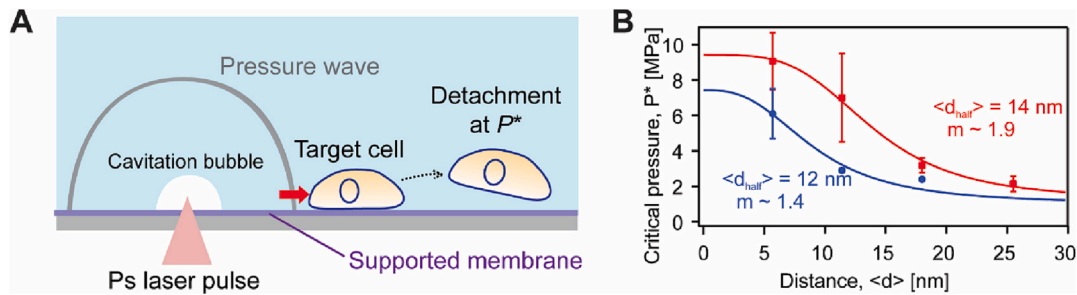
Fig. 4. Novel highthroughput technique for the measurement of cell adhesion strength. (A) Intensive picosecond (ps) laser pulse focused near the surface induces ultrasonic pressure wave (shock wave), which can non-invasively detach the adhered cells. The critical pressure necessary for cell detachment $P*$ can be used as a quantitative measure to mechanical strength of cell adhesion with a high throughput ($N > 100$ cells/h). Adapted from (Yoshikawa et al., 2011). (B) Critical pressure for HSPC detachment $P*$ plotted *versus* $<d>$ for SDF1α (red) and N-cadherin (blue). Solid lines are empirical Hill fits. Adapted from (Burk et al., 2015). (For interpretation of the references to colour in this figure legend, the reader is referred to the web version of this article.)

Sackmann, 1988). As shown in Fig. 4B, the combination with the quantitative *in vitro* niche model can be used to quantitatively compare the mechanical strength of HSPC-niche interactions mediated *via* CXCR4-SDF1α axis, or *via* N-cadherin axis (Burk et al., 2015). This non-invasive assay realized a high-throughput tracking of the change in cell adhesion strength as a function of time, such as the change of cytoadhesion strength of malaria-infected human red blood cells by the growth of *P. falciparum* parasites (Fröhlich et al., 2021; Rieger et al., 2015).

Physical biomarkers for differential functions of chemokines and clinical agents (1): adhesion and migration

As mentioned above, SDF1α-axis represents one of the targets for AML therapy because SDF1α plays key roles in controlling the homing/mobilization of normal HSPCs, or LICs to/from the bone marrow niche (Lapidot et al., 2005). In the bone marrow niche, SDF1α exists as a soluble chemokine in the marrow fluid dictating HSPC migration as well as an immobilized molecule on the mesenchymal stromal cell surface. By quantitative characterization of HSPC behaviors on the membrane-based, surrogate surfaces, Monzel et al. obtained several characteristic
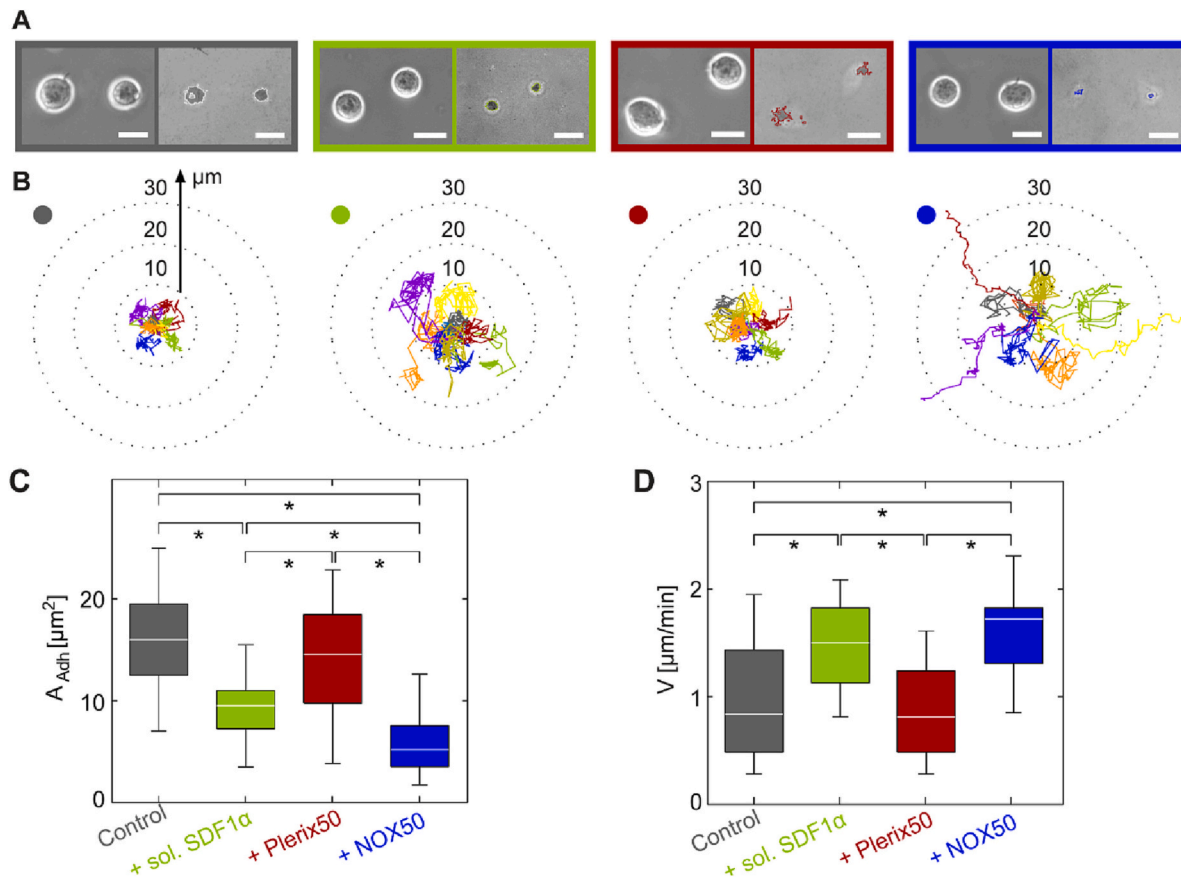

Fig. 5. Modulation of adhesion and migration behaviors of HSPCs by chemokine and clinical agents. (A) Phase contrast (left) and RICM images (right) of HSPC adhering to SDF1α in absence (grey) and presence of sol. SDF1α (green), plerixafor (red, Plerix50) and NOX-A12 (blue, NOX50). Scale bar 5 μm. (B) Migration trajectories of HSPC recorded over 1 h, (C) cell adhesion area A and (D) migration velocity, V on SDF1α-functionalized surrogate surfaces. The colored dots in (B) correspond to the different sample treatments. Significance levels $p < 0.001$ evaluated by Mann-Whitney U test as indicated by (*). Adapted from (Monzel et al., 2018). (For interpretation of the references to colour in this figure legend, the reader is referred to the web version of this article.)

indices that could potentially be used as physical biomarkers for two clinical agents targeting CXCR4-SDF1α axis; plerixafor (AMD3100) from Sigma-Aldrich Co. (St. Louis, USA) and NOX-A12 from NOXXON Pharma AG (Berlin, Germany)) (Monzel et al., 2018). The former is currently used for the mobilization of CD34^{+} cells for autologous transplantations, and the latter, an L-enantiomeric RNA oligonucleotide (called *Spiegelmer*) binds and neutralizes SDF1α (Sayyed et al., 2009). Fig. 5A and B show the adhesion behavior and migration trajectories of HSPC to the surrogate niche model displaying immobilized SDF1α at $<d> = 11$ nm, respectively. In Fig. 5A, four sets of a phase contrast image (left) and a micro-interferometry image (right) of HSPC taken at the following conditions are presented: in the absence of any soluble factors (control, grey) and in the presence of 5 ng/mL SDF1α (green), 50 ng/mL plerixafor/AMD3100 (red), and 50 ng/mL NOX-A12 (blue). Needless to say, the concentrations of soluble factors should be selected carefully and varied systematically for the validation of experimental data. [SDF1α] = 5 ng/mL corresponds to the physiological level in human bone marrow (Burk et al., 2015). Notably, the concentration of plerixafor/AMD3100 (50 ng/mL) is one order of magnitude lower than that used in previous *in vitro* studies, 500 ng/mL (Wuchter et al., 2014). [NOX-A12] = 50 ng/mL (≈ 3.5 nM) is between the IC50 level (≈ 0.3 nM) found in *in vitro* chemotaxis of chronic lymphatic leukemia cells (Hoellenriegel et al., 2014) and the plasma level at which human leukocytes showed an effective mobilization (~ 1 μM) (Vater et al., 2013).

The migration trajectories recorded over 1 h also indicate differential effects of soluble factors (Fig. 5B). The adhesion area per cell (A) calculated from the micro-interferometry image (Fig. 5C) indicates that the presence of plerixafor causes no change in A, which is in contrast to the physiological level of SDF1α causing a distinct decrease. These data strongly suggest that plerixafor does not function as a pure antagonist to the SDF1α-CXCR4 axis, as initially claimed (Uy et al., 2012). In fact, the migration velocity V of plerixafor-treated HSPCs was comparable to the control (Fig. 5D). Conversely, the treatment with NOX-A12 significantly affected the adhesion and migration velocity. The adhesion area of NOX-A12-treated HSPCs is even smaller than that in the presence of physiological SDF1α (Fig. 5C), which can be explained by the neutralization of SDF1α displayed on the surrogate surfaces. A clear increase in the migration velocity caused by SDF1α and NOX-A12 (Fig. 5D) indicates that the competitive binding of soluble SDF1α to CXCR4 and the neutralization of SDF1α by NOX-A12 causes the decrease in A and increase in V. These data are in line with the force measurements utilizing shockwaves, where the presence of soluble SDF1α caused a decrease in the critical pressure for cell detachment by a factor of two (Burk et al., 2015). The direct interference of SDF1α-CXCR4 axis by NOX-A12 was further verified by the comparison of A and V values for HSPCs nested on N-cadherin-functionalized surfaces, showing no detectable difference (Monzel et al., 2018).

Physical biomarkers for differential functions of chemokines and clinical agents (2): spatio-temporal dynamics

For migration of HSPCs from the bone marrow niche, a continuous symmetry breaking of the respective HSPC is a prerequisite before detachment. Deformation of an initially round and hence symmetric cell leads to an emergence of higher modes of deformations, such as elliptic deformation ($m = 2$) and triangular deformation ($m = 3$), which enables the cell to undergo directional motion. In order to deform, cells need to adhere to the niche surface and generate active forces. From this context, the active deformation is connecting the adhesion and migration of HSPCs. The deformation of a biological cell is an active process accompanied by energy dissipation *via* remodeling of cytoskeletons and re-organization of cell membranes, where focal adhesions act as biochemical reaction hubs to logistically recruit a variety of molecules (Sackmann and Tanaka, 2021). Although the active deformation of cells phenomenologically seems random and stochastic, cells often show characteristic spatio-temporal patterns because deformation is tightly

coupled to the biochemical reactions that are often oscillatory due to the involvement of negative feedback loop (Pigolotti et al., 2007; Nguyen, 2012). For example, human hematopoietic stem cells exhibits a periodic deformation every 5 min (Burk et al., 2015; Ohta et al., 2018), whereas a slime mold *D. discoideum* shows an excitable deformation every 2–4 min (Li et al., 2008; Maeda et al., 2008).

To extract the characteristic spatio-temporal deformation patterns, the periphery of a cell was determined based on a pixel intensity threshold (Fig. 6A). The radial distance from the center of mass to the periphery is plotted in a polar coordinate over time (Fig. 6B). For example, the control HSPC (grey) shows strong signals at $\theta = 0$ and $\pm 180°$, suggesting that the cell linearly deforms in a persistent manner. Because the "radial distance maps" are noisier in the presence of SDF1α and clinical agents, the shape deformation should be analyzed in a Fourier space. The Fourier transform of deformation, c_m, is represented as a function of mode m, yielding the power spectrum (Partin et al., 1989; Lamas-Murua et al., 2018):

$$\widehat{\Gamma}_m = \frac{\langle c_m c_{m-} \rangle}{\sum_m \langle c_m c_{m-} \rangle}.$$

This enables us to identify the predominant mode of deformation that HSPC dissipates energy. The power spectrum of HSPCs (Fig. 6C) is dominated by $m = 2$ and $m = 3$, indicating that HSPCs dissipate energy by undergoing elliptic and triangular deformation predominantly. Minor contributions of higher mode deformation ($m \geq 4$) can be attributed to the fact that HSPCs are more compact and less deformable compared to cancer cells (Kaindl et al., 2012). Fig. 5C shows the sum of
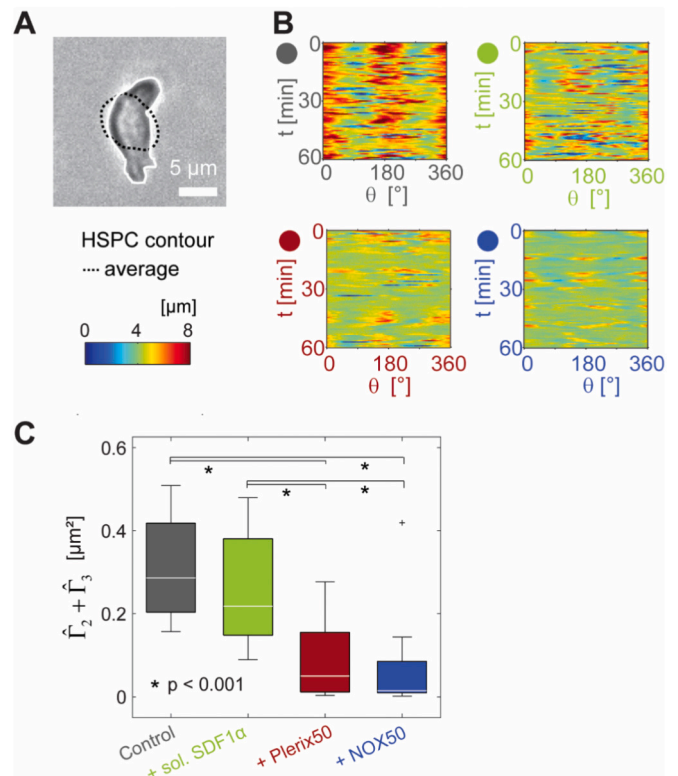

Fig. 6. Modulation of spatio-temporal dynamics of HSPCs by chemokine and clinical agents. (A) Radial distance between the center of mass and cell contour is recorded during the live-cell imaging. (B) Deformation maps of HSPC deformation over time in absence and presence of soluble SDF1α, plerixafor (Plerix50) or NOX-A12 (NOX50) for HSPC on SDF1α functionalized substrates. Scale bar 5 μm. (C) Total power of cell deformation from $m = 2$ and 3, $\widehat{\Gamma}_2 + \widehat{\Gamma}_3$. Significance levels according to Mann-Whitney U test as indicated by (*). Adapted from (Monzel et al., 2018).

A Self-archived copy in
Kyoto University Research Information Repository
https://repository.kulib.kyoto-u.ac.jp

京都大学学術情報リポジトリ
KURENAI 紅
Kyoto University Research Information Repository

powers corresponding to the deformation $m = 2$ and 3, $\widehat{\Gamma_2} + \widehat{\Gamma_3}$, correspponding to the total energy consumption by deformation (Partin et al., 1989). Remarkably, both plerixafor and NOX-A12 resulted in a significant reduction of the energy consumption than SDF1α, which seems to reflect their differential effects on biochemical reactions inside the cells. For example, it is known that the administration of SDF1α suppresses cAMP release, while plerixafor leads to a sustained cAMP release (Gao et al., 2021).

Thoma et al. further extended this strategy to investigate another clinical agent ADH-1 on the adhesion, migration and dynamic deformation of HSPCs (Thoma, 2022). ADH-1, also called exherin (Courtesy of Dr. William Peters, Adherex Technologies, USA), is a cyclic pentapeptide that binds to and block N-cadherin. It has been shown that ADH-1 enhances the antitumor effects of cytotoxic therapy and disrupts cancerous vasculatures by interrupting homophilic N-cadherin interactions (Augustine et al., 2008; Beasley et al., 2011; Yarom et al., 2013). Therefore, the impact of ADH-1 was investigated on the membrane-based surrogate surfaces functionalized with N-cadherin. The treatment with 0.5 μg/mL ADH-1 resulted in a decrease in adhesion area A_{adh} almost by a factor of two, and reduced P^* by a factor of 1.5. Remarkably, the active deformation of HSPC was significantly damped by ADH-1 treatment, characterized by a decrease in $\widehat{\Gamma_2} + \widehat{\Gamma_3}$ by a factor of two, resulting in the compaction of migration trajectories (Thoma, 2022). This is distinct from NOX-A12 binding to SDF1α, causing the decrease in A_{adh} and $\widehat{\Gamma_2} + \widehat{\Gamma_3}$, but streching the migration trajectories.

Physical biomarkers for dissecting roles of intrinsic cues

The aforementioned physical biomarkers, adhesion, migration, and active deformation (energy consumption), can be also used to quantitatively evaluate the effects of intrinsic cues, such as gene knockdown (KD) or protein overexpression. Previously, the power spectrum analysis demonstrated that the disrupted polarization and migration of T-cells overexpressing HIV-1 Nef protein is associated with a distinct decrease in the energy consumption by a factor of 4–5, which could not be quantified otherwise (Lamas-Murua et al., 2018). From the context of AML, Pabst et al. reported that the high expression of an adhesion G-protein coupled receptor GPR56 is associated with poor prognosis in AML patients (Pabst et al., 2016). Recently, they dissected the differential roles of GPR56 by the combination of RNA-seq, functional tests and preclinical studies (He et al., 2022). As the suppression of GPR56 significantly hampered the leukemic engraftment in mice, the influence of GPR56 KD on adhesion and migration of leukemic cells has been quantitatively assessed by physical indices. Micro-interferometry showed that GPR56 KD caused a significant decrease in the adhesion area per cell by a factor of almost two, and the shockwave assay indicated that the critical detachment pressure also decreased by 20 % by GPR56 KD. Moreover, the power spectrum analysis demonstrated that the GPR56 also reduced the energy consumption by a factor of two, which seems reasonable because GPR56-induced enhancement of Wnt and on RhoA signaling pathways (He et al., 2022).

These data suggest the potential of physical biomarkers for indexing epigenetic cues, such as aging. Previously, Hennrich et al. reported proteome-wide atlases of age-associated alterations in human HPSCs and niche cells, including mesenchymal stromal cells by sampling human subjects from different age groups (Hennrich et al., 2018). The proteome data indicated the rerouting of glycolytic intermediate towards anabolism, characteristic for the Warburg effect, according to the aging of HSPCs. Intriguingly, aging also modulates the bone marrow niche, resulting in the decrease in the proteins involved in the homing and hence adhesion of HSPCs to the marrow niche, such as SDF1α and VCAM1. Although the influence of aging on the central carbon metabolism was recently investigated by the total glycogen contents, the function of glycolysis-related enzymes and the capacity of glycogen uptake by young and old human HSPCs (Poisa-Beiro et al., 2020; Poisa-

Beiro et al., 2022), a quantitative understanding of the impact of aging on HSPC-niche interactions is not yet defined.

Combination with theoretical models: mathematical biomarkers

The next challenge is to establish integrate physical indices into a mathematical model in order to translate the effect of extrinsic and intrinsic factors into numerical indices. A simple equation for the velocity of center of mass *v*

$$\mathrm{d}v_i/\mathrm{d}t = \gamma v_i - v^2 v_i - aS_{ij}v_j,$$

coupled with equation for the deformation tensor *S* was introduced to describe instability-driven motion for the movement of a spherical droplet, or a circle in a two-dimensional projection (Ohta and Ohkuma, 2009). However, this set of equations with positive constants *γ* and *a* are not appropriate to describe cell migration. For example, the mobility of a migrating cell, which plays an importnat role in the experiments, does not appear explicitly in the above equation. Quite recently a stochastic model extending that in (Ohta and Ohkuma, 2009) has been applied to the galvanotaxis of keratocytes, but no quantative comparison with experiments has been made (Nwogbaga and Camley, 2023).

During the past several decades, several theoretical models for cell migration have been developed. After the 1D model of persistently migrating cells proposed by DiMilla et al. (DiMilla et al., 1991), several theoretical models of cell dynamics have been developed (Aranson, 2016), such as the stochastic model equations (Li et al., 2008; Takagi et al., 2008) or the theory of active 1D gels (Kruse et al., 2006; Carlsson, 2011). However, these models are not able to handle the shape deformation. To represent deformation-driven cell migration, a 2D phase field model including the degrees of freedom for adhesion seems to be a promising approach (Ziebert and Aranson, 2013; Ziebert and Aranson, 2014).

Ohta et al., introduced a dynamical model for the deformation and migration of cells driven by excitable (Ohta et al., 2016) and periodic forces (Ohta et al., 2018). The center of mass velocity *v* is given by

$$v_i = 2\mu S_{jk}T_{jki},$$

where *μ* represents mobility, and S_{jk} and T_{jki} are the second- and third-rank deformation tensors, respectively. Here, the first derivative of the deformation with respect to time is represented by the combination of the relaxation rate κ_{m}, periodic active deformation force g_{m} with noise ξ_{m}, and the nonlinear coupling term between deformation and velocity b_{m} as shown in Fig. 7A, where deformation with the Fourier modes $m = 2$ and 3 (Fig. 6C) is represented by the second- and third-rank deformation tensors, respectively. Using the experimentally determined quantitative indices (physical biomarkers), the dynamic phenotypes of HSPCs on membrane-based niche in the absence and presence of SDF1α can be recapitulated in a quantitative manner. For example, the mobility *μ* can be controlled by precisely adjusting the intermolecular distance between ligand molecules on the surface $<d>$. The trajectories of a migrating cell are displayed in comparison with numerical results of the model in Fig. 7B. As shown in the figure, the migration trajectories in the presence of SDF1α can only be reproduced by parametrizing SDF1α as the nonlinear coupling between the deformation and motion. It is notable that this model is advantageous over commonly used mathematical ones, because the experimentally determined values and theoretical quantities can be compared not only qualitatively but quantitatively. For example, the experimentally determined energy dissipation, $\widehat{\Gamma_2} + \widehat{\Gamma_3}$, quantitatively matches the sum of deformability $\langle s_2^2 \rangle + \langle s_3^2 \rangle$ in theory (Fig. 7C). The spatio-temporal units employed in this model are the average radius of cell (5 μm) for the space unit and the peroodicity of cell deformation (0.5 min) for the time unit, respectively. Fig. 7D further shows the experimentally determined diffusion constants in the absence (blue) and presence (red) of soluble SDF1α, compared with those
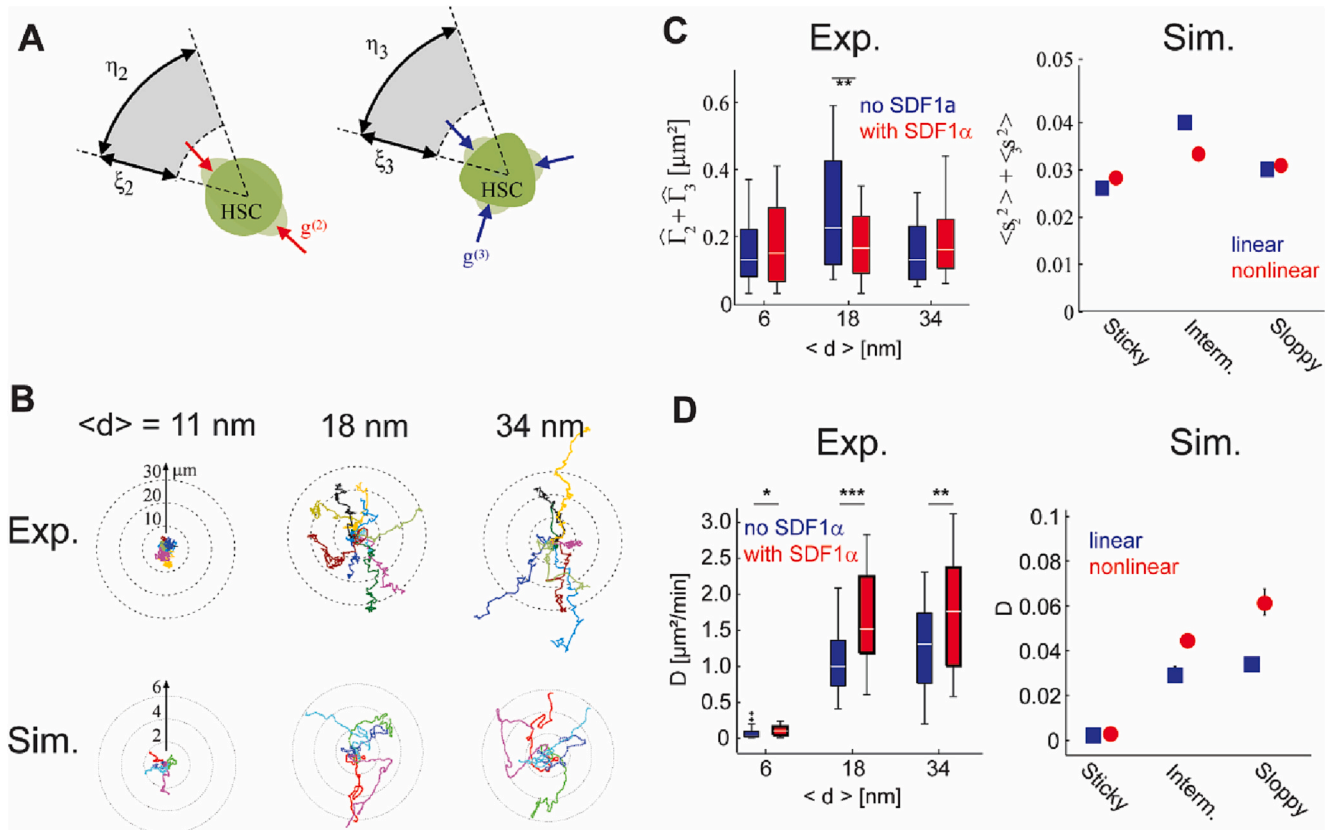
京都大学
KYOTO UNIVERSITY

KURENAI 紅
Kyoto University Research Information Repository

M. Tanaka et al.

Cells & Development 174 (2023) 203845

Fig. 7. Theoretical model of deformation-driven HSPC migration. (A) Modified model of self-propelled, deformable particles (Ohta et al., 2018). Deformation forces $g^{(m)}$, and noises ξ_m and η_m ($m = 2, 3$) acting on the amplitude and the direction of the force, respectively. (B) Influence of soluble chemokine SDF1α on migration trajectories of HSC. The experimental results measured on surrogate surfaces displaying membrane-anchored SDF1α at $<d> = 6$ nm, 18 nm, and 34 nm for 1 h are shown in upper panels (Exp.). The corresponding theoretical trajectories obtained from five independent runs for the non-linear case ($b0 = d0 = 3.0$) are shown in lower panels (Sim.), respectively. The direct comparisons of (C) experimentally determined energy dissipation, $\widehat{\Gamma_2} + \widehat{\Gamma_3}$, and sum of deformability $\langle s_2^2 \rangle + \langle s_3^2 \rangle$ in theory and (D) diffusion constants in the absence (blue) and presence (red) of soluble SDF1α demonstrate the quantitative matching of experiments and simulations both in space and in time. Adapted from (Ohta et al., 2018). (For interpretation of the references to colour in this figure legend, the reader is referred to the web version of this article.)

calculated from numerical data, confirming the excellent agreement between experimental data and simulation results both in space and in time.

Perspectives

As described above, the combination of well-defined, *in vitro* niche models for adhesion and migration of human HSPC and new experimental analytical tools opens a great potential to gain physical, especially dynamic phenotypes of human HSPCs that have not been obtained by commonly used *in vitro* assays. Unique biophysical approaches enable us to dissect the interplay between differential molecular interactions as well as to evaluate the differential effects of clinical agents compared with naturally occurring chemokines on human subjects. It is notable that the "physical biomarkers", quantitative indices representing mechanical forces acting at HSPC-niche interfaces and spatio-temporal dynamics of HSPCs, are fully complementary to the genomic, transcriptomic, and proteomic data, because have no overlap or crosstalk of information. Moreover, direct, quantitative comparison of simulation parameters and non-invasively determined indices provides with a powerful tool to numerically describe the impact of extrinsic cues on primary HSPCs from donors and patients.

One of the promising perspectives is to gain the physical biomarkers that can characterize the effect of intrinsic cues on the HSPCs, such as epigenetic alternation and aging. Recent studies have demonstrated that the aging significantly modulates the protein expression patterns in both

HSPCs and mesenchymal stromal cells, which can be linked to the HSPC-niche interactions and the metabolic pathways. Physical biomarkers and numerical simulations have a potential not only to identify the correlation but also to unravel the causality connecting the aging-related gene modification and the HSPC functions. As our theoretical simulations does not include the biochemical reactions and signaling pathways, the combination of phase field-type simulations and defined mouse models will be complementary.

Data availability

Data will be made available on request.

References

Aiuti, A., Webb, I., Bleul, C., Springer, T., Gutierrez-Ramos, J., 1997. The chemokine SDF-1 is a chemoattractant for human CD34+ hematopoietic progenitor cells and provides a new mechanism to explain the mobilization of CD34+ progenitors to peripheral blood. J. Exp. Med. 185 (1), 111–120.

Aranson, I.S., 2016. Physical Models of Cell Motility. Springer International Publishing, Switzerland.

Augustine, C.K., Yoshimoto, Y., Gupta, M., Zipfel, P.A., Selim, M.A., Febbo, P., Pendergast, A.M., Peters, W.P., Tyler, D.S., 2008. Targeting N-cadherin enhances antitumor activity of cytotoxic therapies in melanoma treatment. Cancer Res. 68 (10), 3777–3784.

Balta, G.S.G., Monzel, C., Kleber, S., Beaudouin, J., Balta, E., Kaindl, T., Chen, S., Gao, L., Thiemann, M., Wirtz, C.R., 2019. 3D cellular architecture modulates tyrosine kinase activity, thereby switching CD95-mediated apoptosis to survival. Cell Rep. 29 (8), 2295–2306 e6.

Bausch, A.R., Moller, W., Sackmann, E., 1999. Measurement of local viscoelasticity and forces in living cells by magnetic tweezers. Biophys. J. 76 (1), 573–579.

Beasley, G.M., Riboh, J.C., Augustine, C.K., Zager, J.S., Hochwald, S.N., Grobmyer, S.R., Peterson, B., Royal, R., Ross, M.I., Tyler, D.S., 2011. Prospective multicenter phase II trial of systemic ADH-1 in combination with melphalan via isolated limb infusion in patients with advanced extremity melanoma. J. Clin. Oncol. 29 (9), 1210–1215.

Bonnet, D., Dick, J.E., 1997. Human acute myeloid leukemia is organized as a hierarchy that originates from a primitive hematopoietic cell. Nat. Med. 3 (7), 730–737.

Boutros, M., Heigwer, F., Laufer, C., 2015. Microscopy-based high-content screening. Cell 163 (6), 1314–1325.

Broxmeyer, H.E., Orschell, C.M., Clapp, D.W., Hangoc, G., Cooper, S., Plett, P.A., Liles, W.C., Li, X., Graham-Evans, B., Campbell, T.B., Calandra, G., Bridger, G., Dale, D.C., Srour, E.F., 2005. Rapid mobilization of murine and human hematopoietic stem and progenitor cells with AMD3100, a CXCR4 antagonist. J. Exp. Med. 201 (8), 1307.

Burk, A.S., Monzel, C., Yoshikawa, H.Y., Wuchter, P., Saffrich, R., Eckstein, V., Tanaka, M., Ho, A.D., 2015. Quantifying adhesion mechanisms and dynamics of human hematopoietic stem and progenitor cells. Sci. Rep. 5 (1), 1–8.

Calvi, L., Adams, G., Weibrecht, K., Weber, J., Olson, D., Knight, M., Martin, R., Schipani, E., Divieti, P., Bringhurst, F.R., 2003. Osteoblastic cells regulate the haematopoietic stem cell niche. Nature 425 (6960), 841–846.

Carlsson, A.E., 2011. Mechanisms of cell propulsion by active stresses. New J. Phys. 13 (7), 073009.

Cheng, J., Schmitt, M., Wuchter, P., Buss, E.C., Witzens-Harig, M., Neben, K., Hundemer, M., Hillengass, J., Alexi, R., Goldschmidt, H., Chen, B.A., Ho, A.D., Schmitt, A., 2015. Plerixafor is effective given either preemptively or as a rescue strategy in poor stem cell mobilizing patients with multiple myeloma. Transfusion 55 (2), 275–283.

Copelan, E.A., 2006. Hematopoietic stem-cell transplantation. N. Engl. J. Med. 354 (17), 1813–1826.

Dar, A., Goichberg, P., Shinder, V., Kalinkovich, A., Kollet, O., Netzer, N., Margalit, R., Zsak, M., Nagler, A., Hardan, I., 2005. Chemokine receptor CXCR4–dependent internalization and resecretion of functional chemokine SDF-1 by bone marrow endothelial and stromal cells. Nat. Immunol. 6 (10), 1038–1046.

DiMilla, P.A., Barbee, K., Lauffenburger, D.A., 1991. Mathematical model for the effects of adhesion and mechanics on cell migration speed. Biophys. J. 60 (1), 15–37.

Ding, L., Saunders, T.L., Enikolopov, G., Morrison, S.J., 2012. Endothelial and perivascular cells maintain haematopoietic stem cells. Nature 481 (7382), 457–462.

DiPersio, J.F., Stadtmauer, E.A., Nademanee, A., Micallef, I.N., Stiff, P.J., Kaufman, J.L., Maziarz, R.T., Hosing, C., Fruehauf, S., Horwitz, M., Cooper, D., Bridger, G., Calandra, G., 2009. Plerixafor and G-CSF versus placebo and G-CSF to mobilize hematopoietic stem cells for autologous stem cell transplantation in patients with multiple myeloma. Blood 113 (23), 5720–5726.

Duong, H.K., Savani, B.N., Copelan, E., Devine, S., Costa, L.J., Wingard, J.R., Shaughnessy, P., Majhail, N., Perales, M.A., Cutler, C.S., Bensinger, W., Litzow, M.R., Mohty, M., Champlin, R.E., Leather, H., Giralt, S., Carpenter, P.A., 2014. Peripheral blood progenitor cell mobilization for autologous and allogeneic hematopoietic cell transplantation: guidelines from the American Society for Blood and Marrow Transplantation. Biol. Blood Marrow Transplant. 20 (9), 1262–1273.

Engelhardt, H., Sackmann, E., 1988. On the measurement of shear elastic-moduli and viscosities of erythrocyte plasma-membranes by transient deformation in high-frequency electric-fields. Biophys. J. 54 (3), 495–508.

Evans, E., Ritchie, K., Merkel, R., 1995. Sensitive force technique to probe molecular adhesion and structural linkages at biological interfaces. Biophys. J. 68 (6), 2580–2587.

Finer, J.T., Simmons, R.M., Spudich, J.A., 1994. Single myosin molecule mechanics - piconewton forces and nanometer steps. Nature 368 (6467), 113–119.

Friedrichs, J., Legate, K.R., Schubert, R., Bharadwaj, M., Werner, C., Müller, D.J., Benoit, M., 2013. A practical guide to quantify cell adhesion using single-cell force spectroscopy. Methods 60 (2), 169–178.

Fröhlich, B., Dasanna, A.K., Lansche, C., Czajor, J., Sanchez, C.P., Cyrklaff, M., Yamamoto, A., Craig, A., Schwarz, U.S., Lanzer, M., 2021. Functionalized supported membranes for quantifying adhesion of P. Falciparum-infected erythrocytes. Biophys. J. 120 (16), 3315–3328.

Fruehauf, S., Veldwijk, M.R., Seeger, T., Schubert, M., Laufs, S., Topaly, J., Wuchter, P., Dillmann, F., Eckstein, V., Wenz, F., Goldschmidt, H., Ho, A.D., Calandra, G., 2009. A combination of granulocyte-colony-stimulating factor (G-CSF) and plerixafor mobilizes more primitive peripheral blood progenitor cells than G-CSF alone: results of a european phase II study. Cytotherapy 11 (8), 992–1001.

Gao, X., Zhang, D., Xu, C., Li, H., Caron, K.M., Frenette, P.S., 2021. Nociceptive nerves regulate haematopoietic stem cell mobilization. Nature 589 (7843), 591–596.

He, L., Arnold, C., Thoma, J., Rohde, C., Kholmatov, M., Garg, S., Hsiao, C.C., Viol, L., Zhang, K., Sun, R., 2022. CDK7/12/13 inhibition targets an oscillating leukemia stem cell network and synergizes with venetoclax in acute myeloid leukemia. EMBO Mol. Med. 14 (4), e14990.

Hennrich, M.L., Romanov, N., Horn, P., Jaeger, S., Eckstein, V., Steeples, V., Ye, F., Ding, X., Poisa-Beiro, L., Lai, M.C., Lang, B., Boultwood, J., Luft, T., Zaugg, J.B., Pellagatti, A., Bork, P., Aloy, P., Gavin, A.-C., Ho, A.D., 2018. Cell-specific proteome analyses of human bone marrow reveal molecular features of age-dependent functional decline. Nat. Commun. 9 (1), 4004.

Ho, A.D., Wagner, W., 2007. The beauty of asymmetry: asymmetric divisions and self-renewal in the haematopoietic system. Curr. Opin. Hematol. 14 (4), 330–336.

Hoellenriegel, J., Zboralski, D., Maasch, C., Rosin, N.Y., Wierda, W.G., Keating, M.J., Kruschinski, A., Burger, J.A., 2014. The spiegelmer NOX-A12, a novel CXCL12 inhibitor, interferes with chronic lymphocytic leukemia cell motility and causes chemosensitization. Blood 123 (7), 1032–1039.

Hosokawa, K., Arai, F., Yoshihara, H., Iwasaki, H., Hembree, M., Yin, T., Nakamura, Y., Gomei, Y., Takubo, K., Shiama, H., 2010. Cadherin-based adhesion is a potential target for niche manipulation to protect hematopoietic stem cells in adult bone marrow. Cell Stem Cell 6 (3), 194–198.

Ishikawa, F., Yoshida, S., Saito, Y., Hijikata, A., Kitamura, H., Tanaka, S., Nakamura, R., Tanaka, T., Tomiyama, H., Saito, N., Fukata, M., Miyamoto, T., Lyons, B., Ohshima, K., Uchida, N., Taniguchi, S., Ohara, O., Akashi, K., Harada, M., Shultz, L. D., 2007. Chemotherapy-resistant human AML stem cells home to and engraft within the bone-marrow endosteal region. Nat. Biotechnol. 25 (11), 1315–1321.

Kaindl, T., Rieger, H., Kaschel, L.-M., Engel, U., Schmaus, A., Sleeman, J., Tanaka, M., 2012. Spatio-temporal patterns of pancreatic cancer cells expressing CD44 isoforms on supported membranes displaying hyaluronic acid oligomers arrays. PLoS ONE 7 (8), e42991.

Kiel, M.J., Yilmaz, Ö.H., Iwashita, T., Yilmaz, O.H., Terhorst, C., Morrison, S.J., 2005. SLAM family receptors distinguish hematopoietic stem and progenitor cells and reveal endothelial niches for stem cells. Cell 121 (7), 1109–1121.

Kruse, K., Joanny, J.F., Jülicher, F., Prost, J., 2006. Contractility and retrograde flow in lamellipodium motion. Phys. Biol. 3 (2), 130–137.

Lamas-Murua, M., Stolp, B., Kaw, S., Thoma, J., Tsopoulidis, N., Trautz, B., Ambiel, I., Reif, T., Arora, S., Imle, A., 2018. HIV-1 nef disrupts CD4+ T lymphocyte polarity, extravasation, and homing to lymph nodes via its nef-associated kinase complex interface. J. Immunol. 201 (9), 2731–2743.

Lane, S.W., Scadden, D.T., Gilliland, D.G., 2009. The leukemic stem cell niche: current concepts and therapeutic opportunities. Blood 114 (6), 1150–1157.

Lapidot, T., Kollet, O., 2002. The essential roles of the chemokine SDF-1 and its receptor CXCR4 in human stem cell homing and repopulation of transplanted immune-deficient NOD/SCID and NOD/SCID/B2mnull mice. Leukemia 16 (10), 1992–2003.

Lapidot, T., Dar, A., Kollet, O., 2005. How do stem cells find their way home? Blood 106 (6), 1901–1910.

Li, L., Nørrelykke, S.F., Cox, E.C., 2008. Persistent cell motion in the absence of external signals: a search strategy for eukaryotic cells. PloS one 3 (5) e2093-e2093.

Lowenberg, B., Downing, J.R., Burnett, A., 1999. Acute myeloid leukemia. N. Engl. J. Med. 341 (14), 1051–1062.

Ludwig, A., Saffrich, R., Eckstein, V., Bruckner, T., Wagner, W., Ho, A.D., Wuchter, P., 2014. Functional potentials of human hematopoietic progenitor cells are maintained by mesenchymal stromal cells and not impaired by plerixafor. Cytotherapy 16 (1), 111–121.

Maeda, Y.T., Inose, J., Matsuo, M.Y., Iwaya, S., Sano, M., 2008. Ordered patterns of cell shape and orientational correlation during spontaneous cell migration. PloS one 3 (11) e3734-e3734.

McCulloch, E., 1983. Stem Cells in Normal and Leukemic Hemopoiesis (Henry Stratton Lecture, 1982).

Mendelson, A., Frenette, P.S., 2014. Hematopoietic stem cell niche maintenance during homeostasis and regeneration. Nat. Med. 20 (8), 833–846.

Méndez-Ferrer, S., Michurina, T.V., Ferraro, F., Mazloom, A.R., MacArthur, B.D., Lira, S. A., Scadden, D.T., Ma'ayan, A., Enikolopov, G.N., Frenette, P.S., 2010. Mesenchymal and haematopoietic stem cells form a unique bone marrow niche. Nature 466 (7308), 829–834.

Merkel, R., Nassoy, P., Leung, A., Ritchie, K., Evans, E., 1999. Energy landscapes of receptor–ligand bonds explored with dynamic force spectroscopy. Nature 397 (6714), 50–53.

Möhle, R., Bautz, F., Rafii, S., Moore, M.A., Brugger, W., Kanz, L., 1998. The chemokine receptor CXCR-4 is expressed on CD34+ hematopoietic progenitors and leukemic cells and mediates transendothelial migration induced by stromal cell-derived factor-1. Blood 91 (12), 4523–4530.

Monika, B.S., Lalita, S.L., Vaijayanti, P.K., 2012. Mimicking the functional hematopoietic stem cell niche in vitro: recapitulation of marrow physiology by hydrogel-based three-dimensional cultures of mesenchymal stromal cells. Haematologica 97 (5), 651–660.

Monzel, C., Becker, A.S., Saffrich, R., Wuchter, P., Eckstein, V., Ho, A.D., Tanaka, M., 2018. Dynamic cellular phenotyping defines specific mobilization mechanisms of human hematopoietic stem and progenitor cells induced by SDF1α versus synthetic agents. Sci. Rep. 8 (1), 1841.

Moore, K.A., Lemischka, I.R., 2006. Stem cells and their niches. Science 311 (5769), 1880–1885.

Morrison, S.J., Scadden, D.T., 2014. The bone marrow niche for haematopoietic stem cells. Nature 505 (7483), 327–334.

Neuman, K.C., Nagy, A., 2008. Single-molecule force spectroscopy: optical tweezers, magnetic tweezers and atomic force microscopy. Nat. Methods 5 (6), 491–505.

Nguyen, L.K., 2012. Regulation of oscillation dynamics in biochemical systems with dual negative feedback loops. J. R. Soc. Interface 9 (73), 1998–2010.

Nwogbaga, I., Camley, B.A., 2023. Coupling cell shape and velocity leads to oscillation and circling in keratocyte galvanotaxis. Biophys. J. 122 (1), 130–142.

Ohta, T., Ohkuma, T., 2009. Deformable self-propelled particles. Phys. Rev. Lett. 102 (15), 154101.

Ohta, T., Tarama, M., Sano, M., 2016. Simple model of cell crawling. Physica D 318–319, 3–11.

Ohta, T., Monzel, C., Becker, A.S., Ho, A.D., Tanaka, M., 2018. Simple physical model unravels influences of chemokine on shape deformation and migration of human hematopoietic stem cells. Sci. Rep. 8 (1), 10630.

Pabst, C., Bergeron, A., Lavallée, V.-P., Yeh, J., Gendron, P., Norddahl, G.L., Krosl, J., Boivin, I., Deneault, E., Simard, J., 2016. GPR56 identifies primary human acute myeloid leukemia cells with high repopulating potential in vivo. Blood 127 (16), 2018–2027.

Partin, A.W., Schoeniger, J.S., Mohler, J.L., Coffey, D.S., 1989. Fourier analysis of cell motility: correlation of motility with metastatic potential. Proc. Natl. Acad. Sci. 86 (4), 1254–1258.

Passweg, J.R., Baldomero, H., Bader, P., Bonini, C., Cesaro, S., Dreger, P., Duarte, R.F., Dufour, C., Kuball, J., Farge-Bancel, D., Gennery, A., Kroger, N., Lanza, F., Nagler, A., Sureda, A., Mohty, M., 2016. Hematopoietic stem cell transplantation in Europe 2014: more than 40 000 transplants annually. Bone Marrow Transplant. 51 (6), 786–792.

Peled, A., Grabovsky, V., Habler, L., Sandbank, J., Arenzana-Seisdedos, F., Petit, I., Ben-Hur, H., Lapidot, T., Alon, R., 1999. The chemokine SDF-1 stimulates integrin-mediated arrest of CD34+ cells on vascular endothelium under shear flow. J. Clin. Investig. 104 (9), 1199.

Petit, I., Szyper-Kravitz, M., Nagler, A., Lahav, M., Peled, A., Habler, L., Ponomaryov, T., Taichman, R.S., Arenzana-Seisdedos, F., Fujii, N., Sandbank, J., Zipori, D., Lapidot, T., 2002. G-CSF induces stem cell mobilization by decreasing bone marrow SDF-1 and up-regulating CXCR4. Nat. Immunol. 3 (7), 687–694.

Pigolotti, S., Krishna, S., Jensen, M.H., 2007. Oscillation patterns in negative feedback loops. Proc. Natl. Acad. Sci. 104 (16), 6533–6537.

Poisa-Beiro, L., Thoma, J., Landry, J., Sauer, S., Yamamoto, A., Eckstein, V., Romanov, N., Raffel, S., Hoffmann, G.F., Bork, P., Benes, V., Gavin, A.-C., Tanaka, M., Ho, A.D., 2020. Glycogen accumulation, central carbon metabolism, and aging of hematopoietic stem and progenitor cells. Sci. Rep. 10 (1), 11597.

Poisa-Beiro, L., Landry, J.J.M., Raffel, S., Tanaka, M., Zaugg, J., Gavin, A.-C., Ho, A.D., 2022. Glucose metabolism and aging of hematopoietic stem and progenitor cells. Int. J. Mol. Sci. 23 (6), 3028.

Ponomaryov, T., Peled, A., Petit, I., Taichman, R.S., Habler, L., Sandbank, J., Arenzana-Seisdedos, F., Magerus, A., Caruz, A., Fujii, N., 2000. Induction of the chemokine stromal-derived factor-1 following DNA damage improves human stem cell function. J. Clin. Invest. 106 (11), 1331–1339.

Pusic, I., DiPersio, J.F., 2010. Update on clinical experience with AMD3100, an SDF-1/CXCL12–CXCR4 inhibitor, in mobilization of hematopoietic stem and progenitor cells. Curr. Opin. Hematol. 17 (4), 319–326.

Rieger, H., Yoshikawa, H.Y., Quadt, K., Nielsen, M.A., Sanchez, C.P., Salanti, A., Tanaka, M., Lanzer, M., 2015. Cytoadhesion of plasmodium falciparum–infected erythrocytes to chondroitin-4-sulfate is cooperative and shear enhanced. Blood 125 (2), 383–391.

Sackmann, E., 1996. Supported membranes: scientific and practical applications. Science 271 (5245), 43–48.

Sackmann, E., Tanaka, M., 2021. Critical role of lipid membranes in polarization and migration of cells: a biophysical view. Biophys. Rev. 13 (1), 123–138.

Sayyed, S.G., Hägele, H., Kulkarni, O.P., Endlich, K., Segerer, S., Eulberg, D., Klussmann, S., Anders, H.-J., 2009. Podocytes produce homeostatic chemokine stromal cell-derived factor-1/CXCL12, which contributes to glomerulosclerosis, podocyte loss and albuminuria in a mouse model of type 2 diabetes. Diabetologia 52 (11), 2445–2454.

Shao, J.-Y., Xu, G., Guo, P., 2004. Quantifying cell-adhesion strength with micropipette manipulation: principle and application. FBL 9 (3), 2183–2191.

Sung, K.-L., Sung, L.A., Crimmins, M., Burakoff, S.J., Chien, S., 1986. Determination of junction avidity of cytolytic T cell and target cell. Science 234 (4782), 1405–1408.

Takagi, H., Sato, M.J., Yanagida, T., Ueda, M., 2008. Functional analysis of spontaneous cell movement under different physiological conditions. PLOS ONE 3 (7), e2648.

Tanaka, M., 2019. In: In Vitro Dynamic Phenotyping for Testing Novel Mobilizing Agents, Stem Cell Mobilization: Methods and Protocols, pp. 11–27.

Tanaka, M., Sackmann, E., 2005. Polymer-supported membranes as models of the cell surface. Nature 437 (7059), 656–663.

Thoma, J., 2022. Electrostatics, Mechanics, and Dynamics of Biological Interfaces at and out of Equilibrium.

Thoumine, O., Kocian, P., Kottelat, A., Meister, J.-J., 2000. Short-term binding of fibroblasts to fibronectin: optical tweezers experiments and probabilistic analysis. Eur. Biophys. J. 29, 398–408.

To, L.B., Haylock, D.N., Simmons, P.J., Juttner, C.A., 1997. The biology and clinical uses of blood stem cells. Blood 89 (7), 2233.

Uy, G.L., Rettig, M.P., Motabi, I.H., McFarland, K., Trinkaus, K.M., Hladnik, L.M., Kulkarni, S., Abboud, C.N., Cashen, A.F., Stockerl-Goldstein, K.E., Vij, R., Westervelt, P., DiPersio, J.F., 2012. A phase 1/2 study of chemosensitization with the CXCR4 antagonist plerixafor in relapsed or refractory acute myeloid leukemia. Blood 119 (17), 3917–3924.

Valent, P., Bonnet, D., De Maria, R., Lapidot, T., Copland, M., Melo, J.V., Chomienne, C., Ishikawa, F., Schuringa, J.J., Stassi, G., 2012. Cancer stem cell definitions and terminology: the devil is in the details. Nat. Rev. Cancer 12 (11), 767–775.

Vater, A., Sahlmann, J., Kröger, N., Zöllner, S., Lioznov, M., Maasch, C., Buchner, K., Vossmeyer, D., Schwoebel, F., Purschke, W.G., Vonhoff, S., Kruschinski, A., Hübel, K., Humphrey, M., Klussmann, S., Fliegert, F., 2013. Hematopoietic stem and progenitor cell mobilization in mice and humans by a first-in-class Mirror-image oligonucleotide inhibitor of CXCL12. Clin. Pharmacol. Ther. 94 (1), 150–157.

Voermans, C., Gerritsen, W.R., Von Dem Borne, A.E.K., Van Der Schoot, C.E., 1999. Increased migration of cord blood-derived CD34+ cells, as compared to bone marrow and mobilized peripheral blood CD34+ cells across uncoated or fibronectin-coated filters. Exp. Hematol. 27 (12), 1806–1814.

Wagner, W., Wein, F., Roderburg, C., Saffrich, R., Faber, A., Krause, U., Schubert, M., Benes, V., Eckstein, V., Maul, H., 2007. Adhesion of hematopoietic progenitor cells to human mesenchymal stem cells as a model for cell– cell interaction. Exp. Hematol. 35 (2), 314–325.

Walenda, T., Bork, S., Horn, P., Wein, F., Saffrich, R., Diehlmann, A., Eckstein, V., Ho, A. D., Wagner, W., 2010. Co-culture with mesenchymal stromal cells increases proliferation and maintenance of haematopoietic progenitor cells. J. Cell. Mol. Med. 14 (1–2), 337–350.

Wein, F., Pietsch, L., Saffrich, R., Wuchter, P., Walenda, T., Bork, S., Horn, P., Diehlmann, A., Eckstein, V., Ho, A.D., 2010. N-cadherin is expressed on human hematopoietic progenitor cells and mediates interaction with human mesenchymal stromal cells. Stem Cell Res. 4 (2), 129–139.

Welte, K., 2014. G-CSF: filgrastim, lenograstim and biosimilars. Expert. Opin. Biol. Ther. 14 (7), 983–993.

Wuchter, P., Ran, D., Bruckner, T., Schmitt, T., Witzens-Harig, M., Neben, K., Goldschmidt, H., Ho, A.D., 2010. Poor mobilization of hematopoietic stem cells-definitions, incidence, risk factors, and impact on outcome of autologous transplantation. Biol. Blood Marrow Transplant. 16 (4), 490–499.

Wuchter, P., Leinweber, C., Saffrich, R., Hanke, M., Eckstein, V., Ho, A.D., Grunze, M., Rosenhahn, A., 2014. Plerixafor induces the rapid and transient release of stromal cell-derived factor-1 alpha from human mesenchymal stromal cells and influences the migration behavior of human hematopoietic progenitor cells. Cell Tissue Res. 355 (2), 315–326.

Wuchter, P., Diehlmann, A., Klüter, H., 2022. Closer to nature: the role of MSCs in recreating the microenvironment of the hematopoietic stem cell niche in vitro. Transfus. Med. Hemother. 49 (4), 258–267.

Yamamoto, A., Mishima, S., Maruyama, N., Sumita, M., 1998. A new technique for direct measurement of the shear force necessary to detach a cell from a material. Biomaterials 19 (7–9), 871–879.

Yarom, N., Stewart, D., Malik, R., Wells, J., Avruch, L., Jonker, D.J., 2013. Phase I clinical trial of exherin (ADH-1) in patients with advanced solid tumors. Curr. Clin. Pharmacol. 8 (1), 81–88.

Yoshikawa, H.Y., Rossetti, F.F., Kaufmann, S., Kaindl, T., Madsen, J., Engel, U., Lewis, A. L., Armes, S.P., Tanaka, M., 2011. Quantitative evaluation of mechanosensing of cells on dynamically tunable hydrogels. J. Am. Chem. Soc. 133 (5), 1367–1374.

Zhang, J., Niu, C., Ye, L., Huang, H., 2003. Identification of the haematopoietic stem cell niche and control of the niche size. Nature 425 (6960), 836.

Ziebert, F., Aranson, I.S., 2013. Effects of adhesion dynamics and substrate compliance on the shape and motility of crawling cells. PloS one 8 (5) e64511-e64511.

Ziebert, F., Aranson, I.S., 2014. Modular approach for modeling cell motility. Eur Phys J Spec Top 223 (7), 1265–1277.